Spatiotemporal Consistency of Local Neural Activities: A New Imaging Measure for Functional MRI Data

Li Dong, PhD,[1,2] Cheng Luo, PhD,[1,2] Weifang Cao, PhD,[1,2] Rui Zhang, PhD,[1,2] Jinnan Gong, PhD,[1,2] Diankun Gong, PhD,[1,2] and Dezhong Yao, PhD[1,2]*

Purpose: To characterize the local consistency by integrating temporal and spatial information in the local region using functional magnetic resonance imaging (fMRI).
Materials and Methods: One simulation was implemented to explain the definition of FOur-dimensional (spatiotemporal) Consistency of local neural Activities (FOCA). Then three experiments included resting state data (33 subjects), resting state reproducibility data (16 subjects), and event state data (motor execution task, 26 subjects) were designed. Finally, FOCA were respectively analyzed using statistical analysis methods, such as one-sample *t*-test and paired *t*-test, etc.
Results: During resting state (Experiment 1), the FOCA values ($P < 0.05$, family-wise error [FWE] corrected, voxel size >621 mm^3) were found to be distinct at the bilateral inferior frontal gyrus, middle frontal gyrus, angular gyrus, and precuneus/cuneus. In Experiment 2 (reproducibility), a high degree of consistency within subjects (correlation ≈ 0.8) and between subjects (correlation ≈ 0.6) of FOCA were obtained. Comparing event with resting state in Experiment 3, enhanced FOCA ($P < 0.05$, FWE-corrected, voxel size >621 mm^3) was observed mainly in the precentral gyrus and lingual gyrus.
Conclusion: These findings suggest that FOCA has the potential to provide further information that will help to better understand brain function in neural imaging.

J. MAGN. RESON. IMAGING 2014;00:000–000.

Functional connectivity among distributed brain regions in the resting state has been widely studied in order to represent the human brain connectome [1] by analyzing spontaneous blood oxygenation level-dependent (BOLD) fluctuations of brain activity measured with functional magnetic resonance imaging (fMRI).[2–4] While most studies have focused on the functional connectivity between different brain regions, the local coherence of a region in the temporal domain has also been examined by numerous studies in recent years. Functional synchrony of the hippocampus in Alzheimer's disease was originally quantified as the mean of the cross-correlation coefficients of spontaneous low frequency (COSLOF).[5] Zang et al [7] proposed a regional homogeneity (ReHo) measure, which was calculated by Kendall's coefficient of concordance (KCC),[6] of a time series per voxel with those of its nearest 26 neighbors. Similarly, with Pearson's correlation, a measure of integrated local correlation (ILC) was introduced to assess the local coherence in fMRI data.[8] More recently, a novel measurement, named local functional connectivity density (local FCD), was proposed to characterize the functional homogeneity in fMRI data.[9]

Each of the above-mentioned measures has their respective strengths and weaknesses in assessing the consistency of temporal fluctuations in local regions. As a rank-based approach, ReHo is robust against noise and is largely free of parametric settings and priori knowledge regarding hemodynamic models.[7,10] However, because KCC is sensitive to the

View this article online at wileyonlinelibrary.com. DOI: 10.1002/jmri.24831

Received Sep 9, 2014, Accepted for publication Dec 5, 2014.

*Address reprint requests to: D.Y., Key Laboratory for NeuroInformation of Ministry of Education, School of Life Science and Technology, University of Electronic Science and Technology of China, Chengdu, 610054, P.R. China. E-mail: dyao@uestc.edu.cn

From the [1]Key Laboratory for NeuroInformation of Ministry of Education, School of Life Science and Technology, University of Electronic Science and Technology of China, Chengdu, P.R. China; and [2]Center for Information in BioMedicine, University of Electronic Science and Technology of China, Chengdu, P.R. China.

Additional Supporting Information may be found in the online version of this article.

number of voxels in the neighboring region, ReHo may be indirectly dependent on image resolution. In an attempt to solve this problem, ILC, which integrates the spatial correlation function, is effectively independent of image resolution and is tissue-specific for gray matter and white matter; however, due to the inherent correlation that is nonnegligible in the data, a correction approach is required before calculating the ILC.[8] This uncertain risk may reduce the potential applications of ILC for uncovering brain function. In addition, local FCD demonstrates its superiority to uncover the distribution hubs in the human brain [9]; however, due to the restriction of the calculation to the local functional connectivity cluster, the local FCD may face practical problems during practical choices of the key parameter settings (thresholds of connectivity and signal-to-noise ratios). All these measures emphasize the temporal consistency in the local region; however, they ignore the effect of spatial correlation in the local region in neighboring time. This meaningful information may be useful for functional brain imaging and may increase our understanding of brain function. Therefore, we hypothesized that local functional brain consistency in the resting state could contain two aspects: a temporal correlation between voxels and a local spatial correlation between neighboring timepoints. And we proposed a new measure, named FOur-dimensional (spatiotemporal) Consistency of local neural Activities (FOCA), to characterize the local consistency by integrating temporal and spatial information in the local region. Additionally, we hypothesized that FOCA could be modulated in pertinent tasks.

Materials and Methods

Definition of FOCA

For image data, a time series of a given voxel with those of its nearest neighbors (26 voxels) can be obtained (Fig. 1a), and a FOCA value assigned to the given voxel can be calculated by the following procedure (Fig. 1b). In the temporal correlation aspect, C_t is defined as the mean of the cross-correlation coefficients of the local voxels and is given in the equation:

$$C_t = \left| \frac{\sum_{i<j}^{N} r_{ij}^t}{N} \right|; N = \frac{k(k-1)}{2} \quad (1)$$

where r^t_{ij} is Pearson's correlation coefficient between voxel i and voxel j, and k is the number of voxels in the local region (27 voxels). On the other hand, for the local spatial distribution in the m-th timepoint, a spatial correlation between distributions in the neighboring timepoint is defined as following:

$$\bar{r}^s_m = \frac{r^s_{m,m-1} + r^s_{m,m+1}}{2} \quad (2)$$

where r is Pearson's correlation coefficient and m is the m-th timepoint. The mean spatial correlation (C_s) across all timepoints is given in the equation:

$$C_s = \left| \frac{\sum_{m=1}^{N_t} \bar{r}^s_m}{N_t} \right| \quad (3)$$

where N_t is the number of timepoints. Then (Fig. 1c), the FOCA value is defined as:

$$FOCA = C_t * C_s \quad (4)$$

Finally, the FOCA value for every voxel can be calculated by Eq. (4) to form FOCA maps. In order to reduce the effect of individual variability, we also normalized the FOCA value of each voxel by dividing it by the mean FOCA of the whole brain for each subject, that is:

$$FOCA_{norm} = \frac{FOCA}{mean(FOCA)} \quad (5)$$

In addition, based on the aforementioned definition of FOCA, a simulation was designed to explain the hypothesis of spatiotemporal consistency in a local region (Supplementary Material A).

Real Data Acquisition

Healthy, right-handed adults participated in the experiments and signed written informed consent. The study was approved by the Ethics Committee of University of Electronic Science and Technology of China (UESTC). All participants had no history of substance abuse, neurological or psychiatric disorders, and were scanned on a 3.0T scanner (GE Discovery MR750, Milwaukee, WI) at the MRI research center of UESTC.

In Experiment 1 the resting state echo planar imaging runs were collected for 33 subjects (16 females / 17 males, mean age ± standard deviation [SD]: 21.5 ± 2.7 years, age range: 17–25 years). The scan parameters were TR/TE = 2000/30 msec; flip angle = 90°; matrix size = 64 × 64; field of view = 24 × 24 cm^2; and thickness/gap = 4/0.4 mm. A total of 255 volumes (32 slices per volumes) were obtained over a 510-second period. Axial anatomical T_1-weighted images were also obtained with a 3D fast-spoiled gradient echo sequence, and the parameters were as follows: TR/TE = 6.008/1.984 msec; flip angle = 9°; matrix size = 256 × 256; field of view = 25.6 × 25.6 cm^2; slice thickness (no gap) = 1 mm. During the scan, all subjects were instructed to close their eyes without falling asleep and without thinking of any particular thing.

In Experiment 2 (testing the reproducibility of FOCA), three repeated resting state scans (Scans 1, 2, and 3) from each subject (a total of 16 subjects, 5 females / 11 males, mean age ± SD: 24.5 ± 1.2 years, age range: 22–27 years) were obtained using the scan parameters described above. Scans 2 and 3 were conducted in a single scan acquisition 20 minutes apart and were obtained 1 year after Scan 1.

In Experiment 3 the MRI data were gathered during a motor execution paradigm. Two runs (left- and right-hand movement) that each consisted of 405 volumes were obtained over an 810-second period. Using the same scan parameters described above, images (containing resting state, task, and T_1-weighted data) were collected in 26 subjects (9 females / 17 males, mean age ± SD: 23.0 ± 2.0 years, age range: 19–26 years).

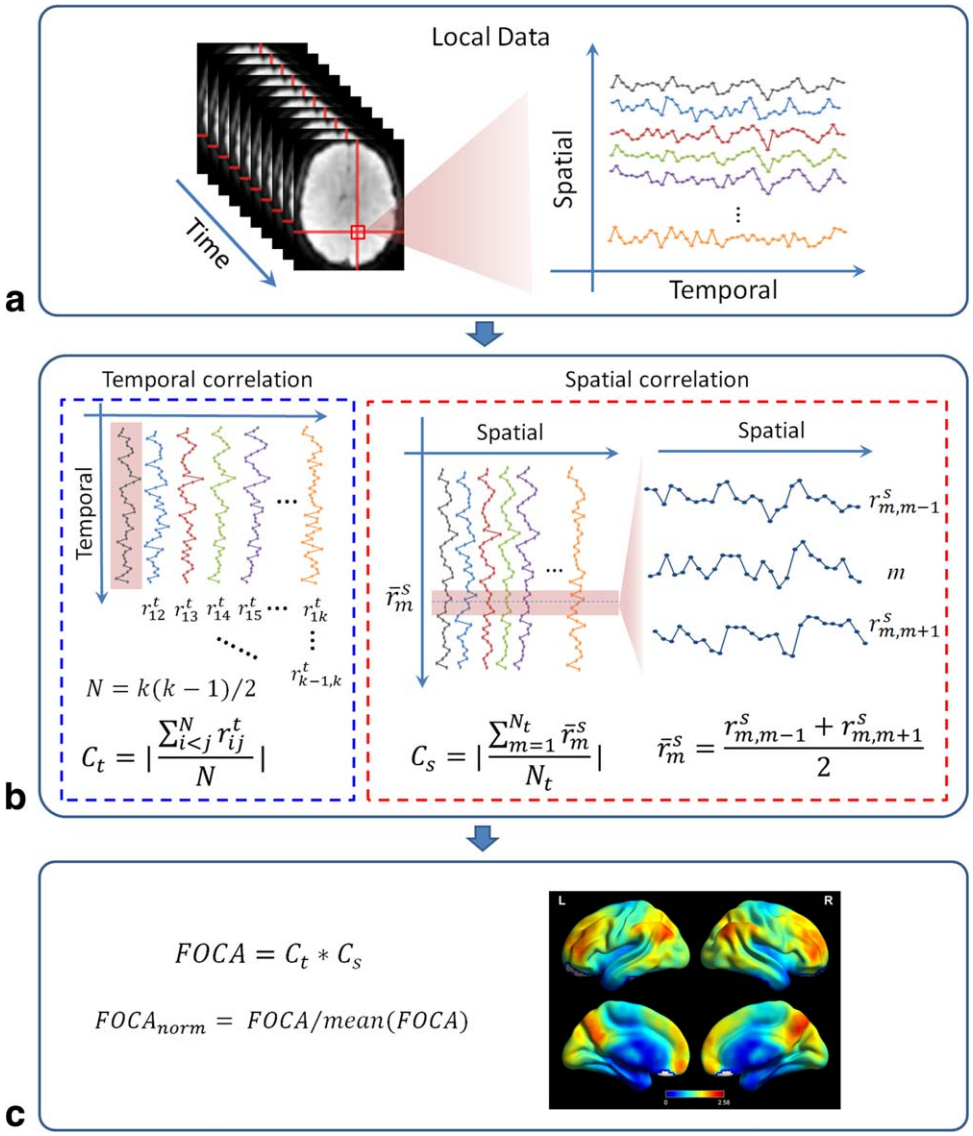

FIGURE 1: Framework of FOCA. a: Spatial and temporal series of a given voxel with those of its nearest neighbors (26 voxels in general) were obtained from fMRI data. b: Temporal correlation (C_t) and spatial correlation (C_s) are calculated in parallel. For C_s (although here we just show window with ±1 TR (m – 1, m, m + 1)), various durations of neighboring time could be considered (for example, from ±1 TR to ±8 TR in the following test). c: FOCA is defined as C_t*C_s and normalized.

Real Data Analysis

In general, the first five volumes were discarded to remove the T_1 saturation effects. Next the conventional preprocessing steps, which were slice time correction, realignment, and spatial normalization (3 × 3 × 3 mm), were analyzed with SPM8. Then the FOCA maps (the toolbox of FOCA is available at http://www.neuro.uestc.edu.cn/FOCA.html with the article) were derived from the functional data preprocessed by regressing out head motion, linear trend, individual white matter (WM), and cerebrospinal fluid (CSF) mean signals (head motion + linear trend + WM/CSF). Prior to the statistical evaluations for the unsmoothed version of FOCA, we performed the same 6-mm FWHM spatial smoothing on normalized FOCA ($FOCA_{norm}$) maps.

In Experiment 1, before analyzing the data with the random effects one-sample *t*-test, the $FOCA_{norm}$ maps generated from the above procedures were subtracted by 1, and the *P*-value threshold was set as $P < 0.05$ (family-wise error [FWE]-corrected, voxel size >621 mm^3). Furthermore, the mean signals were extracted from the adjacent regions (27 voxels) positioned in peak *T*-value clusters of a one-sample *t*-test, and the frequency spectrums of these mean signals were analyzed. To evaluate the influences of neighboring time on FOCA, various durations of neighboring time (from ±1 TR to ±8 TR) were also considered. In addition, to assess the various factors that influence on the intrasession reliability of FOCA, different functional preprocessing procedures, such as regressing out the mean global signal,[11,12] temporal bandpass filtering (which is a phase-insensitive filter between 0.01 and 0.08 Hz [12]) and spatial smoothing (6-mm full-width at half-maximum [FWHM] of an isotropic Gaussian filter), were considered (more details can be seen in Supplementary Material B1). Based on the preprocessed data various measures, such as ReHo (the toolbox is available at http://restfmri.net/forum/REST_V1.8), ILC, and local FCD

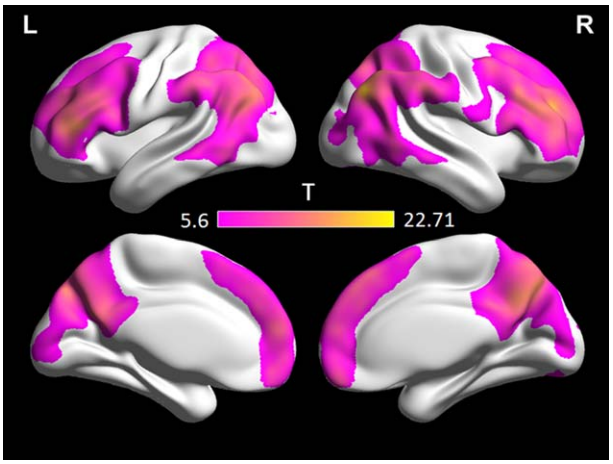

FIGURE 2: T-map of $FOCA_{norm}$ in the resting state using a one-sample *t*-test. Significance was set at $P<0.05$ (FWE-corrected, voxel size >621 mm^3).

(achieved through a custom code) were also considered (more details can be seen in Supplementary Material B2).

In Experiment 2, the data obtained from the repeated resting state scans were used to test the reproducibility and reliability of the tissue-specific pattern in 16 healthy subjects. FOCA maps were generated from all three scans (Scans 1, 2, and 3), and the correlation coefficient between them was used to assess reproducibility and intrasubject variability.[13] The correlation coefficient between subjects in each scan was also calculated to assess the intersubject variability.

Images obtained from the data in Experiment 3 were analyzed to demonstrate the performance of FOCA in event state data. Comparing the $FOCA_{norm}$ maps of the resting state, the $FOCA_{norm}$ maps of the event state were analyzed with paired *t*-tests and the *P*-value threshold was set as $P<0.05$ (FWE-corrected, voxel size >621 mm^3). In addition, the general linear model (GLM) [14] was also conducted on the event state data and the activation revealed by the GLM was compared with the FOCA value.

Results

Characterization of FOCA in the Resting State

Table S1 (Supplementary Material A) shows the simulation results that FOCA emphasized both temporal consistency between voxels and local spatial consistency between neighboring timepoints (mean FOCA values ± SD: 0.91 ± 0.0095). The T-map of $FOCA_{norm}$ in Experiment 1 is shown in Fig. 2, and the significant regions ($P<0.05$, FWE-corrected, voxel size >621 mm^3) revealed by the measure were the middle frontal gyrus (BA10), bilateral angular gyrus (BA39/BA40), precuneus (BA7), bilateral inferior frontal gyrus (BA9/BA46), cuneus (BA19), and fusiform gyrus (BA18/BA19) (Table 1). In Supplementary Material B1, the frequency spectrums (Fig. S4) of all 33 subjects in the regions identified by FOCA demonstrated that the signals in these regions were almost low-frequency signals (<0.08 Hz). Also, the spatial correlation (C_s) and FOCA decreased with increasing neighboring time (Fig. S5). Supplementary Material B1 also shows the influence of different preprocessing steps on C_t, C_s, FOCA, and $FOCA_{norm}$, and different preprocessing steps significantly influencing the $FOCA_{norm}$ value in the whole brain ($F_{4,128}=9.6$, $P<0.05$, FWE-corrected; one-way within-subjects analysis of variance [ANOVA]).

Other measures (ReHo, ILC, and local FCD), which assess the locally functional homogeneity/coherence in the temporal aspect, were also calculated from the data (Supplementary Material B2). The mean FOCA maps and other measures (over 33 subjects) are shown in Fig. S6, and the mean normalized maps of all measures are also displayed. The spatial distributions corresponding to each bar of these histograms are also displayed in Figs. S7–S10. In the white matter and cerebrospinal fluid, the $FOCA_{norm}$ values were mostly below 1. This result indicates that FOCA was sensitive to differences between gray and WM/CSF.

TABLE 1. One-Sample *t*-test Results ($FOCA_{norm}$ maps in the resting state)

MNI coordinates							
x	y	z	L/R	Lobe	Brodmann area	*t*-value	Voxels
30	47	25	R	Middle frontal gyrus	BA10	22.7	15347
45	−73	34	R	Angular gyrus	BA39	21.3	
9	−76	43	R	Precuneus	BA7	16.9	
51	20	28	R	Inferior frontal gyrus	BA9	16.6	
−45	35	10	L	Inferior frontal gyrus	BA46	16.1	
−39	−67	43	L	Angular gyrus	BA39/BA40	15.7	
−3	−79	34	L	Cuneus	BA19	15.3	
−18	−82	−23	L	Fusiform gyrus	BA18/BA19	8.2	69

The significance was set at $P<0.05$ (FWE-corrected).

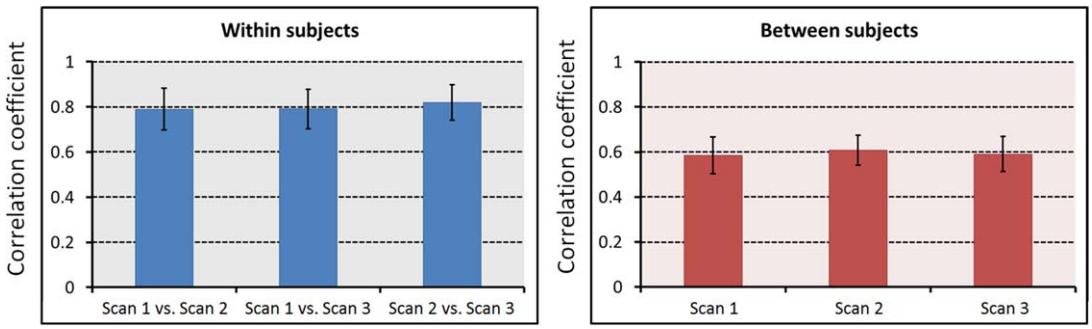

FIGURE 3: Results of FOCA reproducibility. The mean correlation coefficients between FOCA maps obtained from repeated scans (left, 16 pairs) or from subjects in one scan (right, 120 pairs) are demonstrated.

FOCA Reproducibility

Figure 3 shows the mean correlation coefficients between the FOCA maps obtained from repeated scans and from paired subjects in one scan. The mean coefficients (within subjects) between the FOCA maps generated from repeated scans were 0.7898, 0.7905, and 0.8191, corresponding to Scan 1 vs. Scan 2, Scan 1 vs. Scan 3, and Scan 2 vs. Scan 3, respectively. There were no significant differences between correlations of different paired scans. The mean coefficients between subjects in each scan were 0.5853, 0.6082, and 0.5915, corresponding to Scan 1, Scan 2, and Scan 3. There were no significant correlation differences between the two scans. In addition, the spatial distributions of the mean $FOCA_{norm}$ maps (across 16 subjects) in each repeated scan and all scans were extremely similar (Fig. S11 in Supplementary Material C). There is a high degree (~0.8) of consistency within subjects and good consistency (~0.6) between subjects.

FOCA in an Event State

The event state fMRI data were gathered during two motor execution tasks (using the left or right hand) that involved moving the palm up and down. The mean $FOCA_{norm}$ map results (across 26 subjects) during the tasks and the statistical test are shown in Fig. 4. The corresponding maps of temporal correlation (C_t) and spatial correlation (C_s) are also displayed in Fig. S12 (Supplementary Material D). Compared with the resting state, the positive significant regions ($P < 0.05$, FWE-corrected, voxel size >621 mm^3) corresponding to left-hand movement (Table 2) consisted of

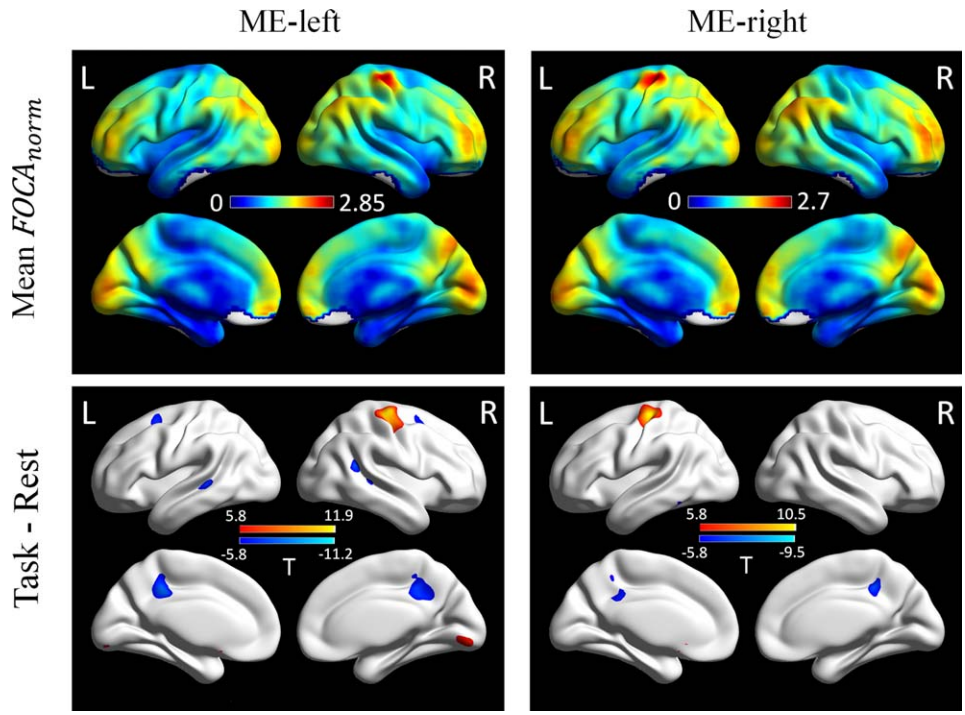

FIGURE 4: Results of $FOCA_{norm}$ and statistical tests ($P < 0.05$, FWE-corrected) during motor execution tasks. Mean $FOCA_{norm}$ maps (26 subjects) generated during left-hand (ME-left) or right-hand (ME-right) movement are shown in the first row. The T-maps of the paired *t*-test between the $FOCA_{norm}$ maps generated from the event state and resting state are also displayed in the second row.

TABLE 2. Paired *t*-test Results From Moving the Left Hand (ME-left) and Moving the Right Hand (ME-right)

Task		MNI coordinates x	y	z	L/R	Lobe	Brodmann area	*t*-value	Voxels
ME-left	Task > rest	36	−21	66	R	Precentral gyrus	BA6	11.91	526
		0	−87	−15		Lingual gyrus	BA18	10.98	313
		−21	−51	−27	L	Cerebelum_6		8.45	42
		−33	−96	0	L	Middle occipital gyrus	BA18	7.37	29
		18	−6	−6	R	Pallidum		7.25	25
	Task < rest	−39	−30	−24	L	Fusiform gyrus	BA20	11.22	56
		48	−15	−27	R	Sub-gyral	BA20	10.13	46
		27	−51	24	R	Precuneus	BA23	9.66	1006
		−12	−39	33	L	Cingulate gyrus	BA31	8.66	
		9	−39	27	R	Posterior cingulate	BA23	8.12	
		−18	9	54	L	Superior frontal gyrus	BA6	8.04	87
		30	12	48	R	Middle frontal gyrus	BA6	7.45	67
		−36	9	45	L	Middle frontal gyrus	BA8	6.69	23
ME-right	Task > rest	−36	−21	60	L	Precentral gyrus	BA4	10.53	437
		−6	15	−15	L	Subcallosal gyrus	BA25	10.31	26
		24	−51	−33	R	Cerebelum_6		8.16	36
		0	−87	−12		Lingual gyrus	BA18	7.57	32
	Task < rest	−18	−48	27	L	Cingulate gyrus	BA31	9.49	358
		18	−42	27	R	Cingulate gyrus	BA31	8.67	191
		27	−51	24	R	Precuneus	BA23	8.66	
		−57	−48	−18	L	Inferior temporal gyrus	BA20	6.74	29

The significance was set at $P < 0.05$ (FWE-corrected).

the right precentral gyrus (BA6), lingual gyrus (BA18), cerebellum, and pallidum. The negative regions consisted of the fusiform gyrus (BA20), precuneus (BA23), cingulate gyrus (BA31), superior frontal gyrus (BA6), and bilateral middle frontal gyrus (BA6/BA8). During right-hand movement (Table 2), the positive significant regions (compared with the resting state, $P < 0.05$, FWE-corrected, voxel size >621 mm^3) were the left precentral gyrus (BA6), cerebellum, and lingual gyrus (BA18). The negative regions consisted of the bilateral cingulate gyrus (BA31), precuneus (BA23), and inferior temporal gyrus (BA20). In addition, the positive regions included in the motor execution-related cortices were similar to the GLM results (Figs. S13–S14 and Tables S2–S3 in Supplementary Material D).

Discussion

In the resting state data, the significant regions revealed by FOCA contained some components of the default mode network (particularly the precuneus, bilateral angular gyrus, and middle frontal gyrus) in which higher regional cerebral blood flow [15] and previous measures have been reported.[7–9] The occipital regions in which higher values of other measures have been reported by previous studies [9,16] were also identified. Furthermore, the frequency spectrums in regions revealed by FOCA demonstrated that the signals in these regions were almost low-frequency, spontaneous activity signals (<0.08 Hz).[3] These findings suggest that spatiotemporal consistency, as measured by FOCA, was a meaningful characteristic of the human brain connectome [1] and may depend on dynamic BOLD responses to neuronal activity and local brain structure.

Removing the global signal [11,12] was not a significant factor and did not significantly alter the FOCA values. This result may be due to the similarity of regressing out the global signal on synchronous signals in the local region, and this effect may not have significantly changed the local coherence. Bandpass temporal filtering between 0.01 Hz and 0.08 Hz [3,12] was always used to remove scanner drift

(<0.01 Hz) [17] and physiological noise generated from respiratory and cardiac functions (>0.1 Hz).[18] However, Davey et al [19] found that temporal filtering may artificially induce temporal correlation connectivity in fMRI resting state data. This effect might have occurred because temporal filtering decreased the temporal variation (high frequency), which then artificially increased the spatial consistency of different times in the local region. Hence, the FOCA maps generated from the data after temporal filtering only partially reflect the specificity of temporal consistency in the local region. Zuo et al [10] found that spatial smoothing may artificially enhance ReHo intensity. In other words, spatial smoothing artificially strengthens temporal consistency in the local region. Therefore, FOCA maps derived from data with spatial smoothing partially reflected the specificity of spatial consistency in the local region, and the specificity of temporal consistency was masked. The performance of FOCA was poor in the RAW data, and the spatiotemporal specificity of consistency in the local region was not well differentiated by FOCA.

Tissue specificity for differences in fMRI physiology and neural processing has been demonstrated in previous studies, and differences between the gray and white matter is one type of tissue specificity.[8,20] However, tissue specificity in the gray matter should be investigated further. In the resting state data, FOCA was not only sensitive to differences between gray and WM/CSF but also showed good tissue specificity within the gray matter. Our results also demonstrated that ReHo [7] was able to discriminate between different gray matter tissues, but ILC may be more sensitive (than ReHo) to differences between gray and white matter.[8] The local FCD data also agreed with previous studies that local FCD demonstrates the distribution of functional hubs in the brain located in the precuneus and occipital cortex.[9] These results demonstrate that each measure has unique strengths and weaknesses for the characterization of the consistency of local neural activity within the human brain.

In the reproducibility data, there was a high degree of consistency within subjects, and the patterns revealed by FOCA were consistent across consecutive resting state scans. Considering that multiple factors (such as age, gender, and state of subjects) may cause FOCA variability between subjects, the consistency across subjects was acceptable. Overall, considering that the reliability of previous fMRI studies typically ranges from 20% to 80%,[9,21] the degree of consistency of FOCA during the resting state is comparable to these studies. FOCA may also be a robust measure for the assessment of spatiotemporal consistency in local brain regions.

In the event state data, compared to the corresponding resting state, primarily positive regions were identified by FOCA consistently related to the motor execution task, which corroborates previous studies.[22–24] These positive regions were also similar to the GLM results. Interestingly, some studies have suggested that interregional connectivity in the motor network does not change under different conditions (resting state vs. event state). In other words, a motor task may not alter the local temporal consistency [8,25]; however, it perhaps changes the local spatial consistency in neighboring time. A task-induced deactivation (TID) has been identified in previous studies and was interpreted as the reallocation of processing resources from areas in which TIDs occurred to areas that have been identified for task performance.[26,27] The negative results may provide further evidence that TIDs exist in normal brain function. Overall, these results demonstrate that the changes in spatiotemporal consistency in a local region reflect the sum brain function to an extent, and FOCA could be a potential measure to capture these changes under different conditions.

One important limitation should be considered for the future use of FOCA. Temporal filtering and spatial smoothing can influence the spatial and temporal correlations in a local region, respectively. Therefore, one strategy in our study was to remove these two steps from the preprocessing procedure. This strategy may increase the requirement of data quality. However, for poor quality data, the spatial correlation (C_s^*) can be calculated from smoothed data (not filtered) and the temporal correlation (C_t^*) can be calculated from filtered data (not smoothed). Then FOCA can be defined as the product of the spatial and temporal correlation ($C_s^* \cdot C_t^*$). In addition, some useful suggestions are also provided. Because the hemodynamic responses of various events overlap in a rapid, event-related design, the application of FOCA in these tasks should be further investigated. Also, a current EPI technique for fast scanning[28,29] perhaps makes it possible to apply FOCA in the rapid event-related task. Furthermore, taking into account that FOCA represents the local spatiotemporal consistency, FOCA may extend our understanding of brain functions and dysfunctions, such as altered spatiotemporal patterns induced by interictal epileptic discharges.[30,31]

In conclusion, this investigation characterized the spatiotemporal 4D consistency in local brain regions. Additionally, we introduced a new local measure, FOCA, to reveal the characteristics of local brain activation. These findings suggest that FOCA may provide additional information that will help in the understanding of brain function.

Acknowledgments

Contract grant sponsor: the 973 project; Contract grant number: 2011CB707803; Contract grant sponsor: National Nature Science Foundation of China; Contract grant numbers: 81271547, 91232725, 81330032, and 81471638; Contract grant sponsor: Program for Changjiang Scholars

and Innovative Research Team; Contract grant number: IRT0910; Contract grant sponsor: Special-Funded Program on National Key Scientific Instruments and Equipment Development of China; Contract grant number: 2013YQ490859; Contract grant sponsor: the 111 project; Contract grant number: B12027.

References

1. Bullmore E, Sporns O. The economy of brain network organization. Nat Rev Neurosci 2012;13:336–349.
2. Biswal B, Yetkin FZ, Haughton VM, Hyde JS. Functional connectivity in the motor cortex of resting human brain using echo-planar MRI. Magn Reson Med 1995;34:537–541.
3. Fox MD, Raichle ME. Spontaneous fluctuations in brain activity observed with functional magnetic resonance imaging. Nat Rev Neurosci 2007;8:700–711.
4. Kelly C, Biswal BB, Craddock RC, Castellanos FX, Milham MP. Characterizing variation in the functional connectome: promise and pitfalls. Trends Cogn Sci 2012;16:181–188.
5. Li SJ, Li Z, Wu G, Zhang MJ, Franczak M, Antuono PG. Alzheimer disease: evaluation of a functional MR imaging index as a marker. Radiology 2002;225:253–259.
6. Kendall MG. Rank correlation methods. New York: Oxford University Press; 1990.
7. Zang Y, Jiang T, Lu Y, He Y, Tian L. Regional homogeneity approach to fMRI data analysis. Neuroimage 2004;22:394–400.
8. Deshpande G, LaConte S, Peltier S, Hu X. Integrated local correlation: a new measure of local coherence in fMRI data. Hum Brain Mapp 2009;30:13–23.
9. Tomasi D, Volkow ND. Functional connectivity density mapping. Proc Natl Acad Sci U S A 2010;107:9885–9890.
10. Zuo XN, Xu T, Jiang L, et al. Toward reliable characterization of functional homogeneity in the human brain: preprocessing, scan duration, imaging resolution and computational space. Neuroimage 2013;65:374–386.
11. Fox MD, Zhang D, Snyder AZ, Raichle ME. The global signal and observed anticorrelated resting state brain networks. J Neurophysiol 2009;101:3270–3283.
12. Fox MD, Snyder AZ, Vincent JL, Corbetta M, Van Essen DC, Raichle ME. The human brain is intrinsically organized into dynamic, anticorrelated functional networks. Proc Natl Acad Sci U S A 2005;102:9673–9678.
13. Strother SC, Lange N, Anderson JR, et al. Activation pattern reproducibility: measuring the effects of group size and data analysis models. Hum Brain Mapp 1997;5:312–316.
14. Friston KJ. Statistical parametric mapping: the analysis of functional brain images. Amsterdam, Boston: Elsevier/Academic Press; 2007.
15. Raichle ME, MacLeod AM, Snyder AZ, Powers WJ, Gusnard DA, Shulman GL. A default mode of brain function. Proc Natl Acad Sci U S A 2001;98:676–682.
16. Wu T, Long X, Zang Y, et al. Regional homogeneity changes in patients with Parkinson's disease. Hum Brain Mapp 2009;30:1502–1510.
17. Bianciardi M, Fukunaga M, van Gelderen P, et al. Sources of functional magnetic resonance imaging signal fluctuations in the human brain at rest: a 7 T study. Magn Reson Imaging 2009;27:1019–1029.
18. Cordes D, Haughton VM, Arfanakis K, et al. Frequencies contributing to functional connectivity in the cerebral cortex in "resting-state" data. AJNR Am J Neuroradiol 2001;22:1326–1333.
19. Davey CE, Grayden DB, Egan GF, Johnston LA. Filtering induces correlation in fMRI resting state data. Neuroimage 2013;64:728–740.
20. Deshpande G, Laconte S, Peltier S, Hu X. Tissue specificity of nonlinear dynamics in baseline fMRI. Magn Reson Med 2006;55:626–632.
21. Aron AR, Gluck MA, Poldrack RA. Long-term test-retest reliability of functional MRI in a classification learning task. Neuroimage 2006;29:1000–1006.
22. Gao Q, Duan X, Chen H. Evaluation of effective connectivity of motor areas during motor imagery and execution using conditional Granger causality. Neuroimage 2011;54:1280–1288.
23. Kansaku K, Muraki S, Umeyama S, et al. Cortical activity in multiple motor areas during sequential finger movements: an application of independent component analysis. Neuroimage 2005;28:669–681.
24. Hanakawa T, Dimyan MA, Hallett M. Motor planning, imagery, and execution in the distributed motor network: a time-course study with functional MRI. Cereb Cortex 2008;18:2775–2788.
25. Morgan VL, Price RR. The effect of sensorimotor activation on functional connectivity mapping with MRI. Magn Reson Imaging 2004;22:1069–1075.
26. McKiernan KA, D'Angelo BR, Kaufman JN, Binder JR. Interrupting the "stream of consciousness": an fMRI investigation. Neuroimage 2006;29:1185–1191.
27. McKiernan KA, Kaufman JN, Kucera-Thompson J, Binder JR. A parametric manipulation of factors affecting task-induced deactivation in functional neuroimaging. J Cogn Neurosci 2003;15:394–408.
28. Feinberg DA, Moeller S, Smith SM, et al. Multiplexed echo planar imaging for sub-second whole brain FMRI and fast diffusion imaging. PLoS One 2010;5:e15710.
29. Boubela RN, Kalcher K, Nasel C, Moser E. Scanning fast and slow: current limitations of 3 Tesla functional MRI and future potential. Front Phys 2014;2:1.
30. Gotman J, Pittau F. Combining EEG and fMRI in the study of epileptic discharges. Epilepsia 2011;52(Suppl 4):38–42.
31. Luo C, An D, Yao D, Gotman J. Patient-specific connectivity pattern of epileptic network in frontal lobe epilepsy. Neuroimage Clin 2014;4:668–675.